RSC Advances

ROYAL SOCIETY OF CHEMISTRY

www.rsc.org/advances

An ink-jet printed surface enhanced Raman scattering paper for food screening.

Wei-Ju Liao,[a] Pradip Kumar Roy,[a] Surojit Chattopadhyay*[a,b]

A printable surface enhanced Raman scattering (SERS) active test strip, with *in-situ* growth of gold nanoparticles on fully untreated paper, is demonstrated to screen for bio-toxins in food below the maximum residue levels in the European Union. The cheap disposable strip on as-purchased printing paper can also be used for SERS mapping of fluorescent dyes.

1 Introduction

Food safety is a glaring global threat following the melamine adulterated infant formula and pet food reported in China, and several incidents involving phthalates in soft drinks, and Maleic acid in rice based food products. Such toxic agents are generally detected in labs using mass spectroscopic, liquid chromatographic or bio-assay techniques. The availability of portable Raman spectrometers, along with noble metal nanoparticle (NP) enhanced Raman scattering opens up possibility for on-site toxic screening via plasmonics. Surface enhanced Raman scattering (SERS) has developed into a frontline tool for chemical analysis, sensing,[1] and identification of a wide range of adsorbate molecules down to the limit of single molecule detection.[2] In many cases sensing was done on labeled molecules.[3] The signal enhancement involves a 10^6 times increase in the Raman scattering (RS) cross-section σ believed to be due to a surface plasmon aided stronger electro-magnetic field at the analyte site, [4] in addition to a possible enhancement through a chemical charge transfer effect.[4] Along with organic and inorganic molecules, SERS is becoming increasingly important for bio-sensing[5, 6] and quality control of food and drinks.[7, 8] In order to have a high sensitivity of detection via SERS, it is imperative to have a good SERS platform containing the metal (Au, Ag) NPs with specific density, size, morphology, and of course the nature of the support on which the AuNPs are dispersed. Au and Ag NPs are prepared through a multitude of processes [9-11] in which a gold or silver containing salt is reduced by citrates, sugars (glucose, fructose and sucrose),[10] or boranes, that work under certain temperatures, with different reaction rates. One common method to synthesize AuNPs is from the reduction of hydrochloroauric acid ($HAuCl_4$), with sodium citrate ($C_6H_5O_7Na_3$). In one of the recent developments, lecithin, a component of human sweat, has been used as a reducing agent to grow AuNPs, at room temperatures, using $HAuCl_4$.[12] Physical vapour deposition methods have also been used to grow Au and Ag NPs.[13, 14]

Solid SERS substrates are very common for such analytical applications we are considering. The advantages of using a solid substrate is that, both top down and bottom up fabrication is possible, of which the former has high precision in controlling the location and dimension of the plasmon generating structures. This is important since previous reports studies lead one to believe that exceedingly small structures and gaps (<10 nm) are required to generate the hot spots typically associated with high SERS activity.[15] These SERS platforms are developed using nanolithography methods,[16] including electron-beam (e-beam) lithography,[17] nanoimprint lithography technique,[18] photo-lithography technique ,[19-22] together with several examples of template based [18] and sputtering methodologies[13, 23] to generate the metallic nano-patterns. Successful fabrication and application of uniform SERS substrates have been demonstrated in commercially available Klarite™ substrates that uses inverted gold pyramidal[16, 24] structures. But these substrates are difficult to use on-site and outside the laboratory for practical constraints of size, flexibility, contamination, and cost. Moreover, the fabrications of these rigid substrates are energy intensive and leave behind substantial waste.

On the other hand, owing to the problems associated with a rigid SERS substrate, researchers have attempted flexible substrates with reasonable success. Flexible SERS substrates can be easily incorporated into spectroscopic assemblies without the requirement of special handling or laboratory environments. Noble metal NPs have been grown on supports including flexible polymers,[25, 26] fibers,[27] carbon nanotubes,[28] and paper.[29] The recent development on flexible SERS substrates use nanoimprint,[30] electrospinning,[31, 32] thermal inkjet technology,[33] shadow mask assisted evaporation,[34] and oblique angle deposition method.[35] The nanoimprinting and electrospinning approach for polymer and nanofiber substrates are either complicated or room temperature incompatible. But not all of these have been used for SERS application presumably due to the strong background Raman signals from the substrate itself, or other prohibitory factors arising out of NP loading density, or background fluorescence.

In this study we demonstrate an *in-situ* growth of AuNPs, on chemically unmodified as-purchased printing paper, using an inkjet printing process to obtain a sensitive SERS paper for analytical purposes of sensing and mapping. With this SERS strip, and a portable Raman spectrometer, loaded with a chemical library, it is possible to demonstrate a high sensitivity screening of toxic food outside the laboratory without the need of any expert handling.

2 Preparation and characterization of the SERS strip

2.1 Preparation of the SERS strip

The preparation of AuNPs on paper uses a bio-ink consisting of a combination of aqueous solution of Lecithin (Acros, Belgium), and Potassium Iodide (KI, 99.5%, Acros, Belgium) mixed in a 1:1 volume ratio. The solution was then injected as an ink into an empty cartridge of an inkjet printer. A computer generated user-defined pattern was printed out on plain A4 paper ($72Kg/m^3$, Taiwan). No hydrophobization of the A4 paper was performed. The pattern is initially invisible to the naked eye, but when immersed in an aqueous solution of $HAuCl_4$ ($HAuCl_4 \bullet 3H_2O$, 99.99%, ACS reagent, Acros, Belgium) at room temperature, the bio-ink reduces the $HAuCl_4$ and *in situ* growth of Au NPs proceed and visible purple patterns develop on the paper signifying the presence of AuNPs. The developing time can be from 2-24 hrs depending on the concentration of the bio-ink and

the $HAuCl_4$. A representative photograph of the SERS strip is shown in Fig. 1 and the procedure to prepare it is shown in Fig. S1(Electronic Supporting Information, ESI†). The colour of the AuNP pads, pink-purple, on the SERS strips depend on the AuNP size and density, and those without AuNPs appear white (Fig. 1a). Fig. 1b shows the SERS strip being developed vis-à-vis a commercial pH paper (green). The printing technique is capable of generating complex patterns as shown in Fig. 1c which is the National Yang Ming University, Taiwan, logo (inset, Fig. 1c). The sharpness of the patterns is governed by the printer head, and diffusion of the reactants on the wet paper. For smaller and sharper patterns, for applications such as blood typing[36], better printers and low wettability paper may be used. The approximate material cost of preparing one such AuNP pad is about 0.1 USD. To control the AuNP density or size, the reactant concentrations had to be changed. In the present case, the reactant concentration varied from 25-75 mM for Lecithin, 2 -10 mM for $HAuCl_4$, but KI concentration was fixed at 100 mM.

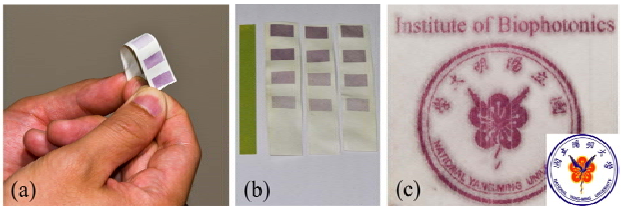

Fig. 1. (a) Optical image of the SERS strip showing purple AuNP patterns on paper. (b) Comparison between commercial pH strips and herein invented SERS strips. (c) Optical image of complex patterns (Logo of National Yang Ming University) using the same technique for printing the SERS strips. Inset in (c) shows the original logo of National Yang Ming University.

Although there are few reports on silver coated paper,[37] the first patterned and printed SERS strips came from I. M. White's group.[38] They used as-grown AgNP solution, whose viscosity is chemically controlled by glycerol, and the 'ink' is introduced into the printer cartridges for printing. This method is technically well controlled, however, more complicated because of the use of centrifugation, filtration and requires chemical treatment for making the cellulose paper hydrophobic. The 'ink' used in these printing processes may clog the printer head, and storage of this ink within the cartridges is challenging. Using a printer with micro electromechanical system (MEMS) based actuation and filtration may partly solve the corrosion or clogging issue, but its industrial sustainability is not known. In addition, the chemicals used in the surface modification process may complicate the spectroscopic background. These steps are redundant in the process described here. The nanoparticle density, controlled by repeated printing in the published report,[38] is apparently larger than our case which we control by the reactant concentration only. The other difference between the published work and this report is that we have used only the common A4 paper for printing as against chromatography paper[38] used previously. There has been a recent report on disposable screen printed SERS assay on solid substrates[39] following basically similar steps, but different chemicals, as described by Yu et al. This report mentioned that a screen printed paper based SERS substrate was the weakest. However, none of these substrates were tested for toxins in real food that have smaller Raman scattering cross-section than dyes such as R6G used in these previously published papers. The problem of millimetre scale paper wrinkling (Fig. 1b) observed here due to long periods of immersion is not a serious problem, since the laser beam of the Raman spectroscopic setup is only a few microns across and data collection is not disturbed once focus is achieved.

2.2 Characterization of the AuNPs

The sensing performance will depend on the AuNP characteristics shown in Fig. 2. SERS signal will increase with the strength of the electric field in the surface plasmons generated in the metal NPs when properly irradiated. The calculations of Garcia-Vidal and Pendry[40] showed that the metal inter-particle spacing (d) contributes more to the enhancement factor in SERS rather than the radius (r) of the metal NPs. They predicted that metal NPs touching each other, in a monolayer, to yield $d=2r$ would produce the highest SERS sensitivity. The morphology of the AuNPs were studied by transmission electron microscopy (TEM, JEOL, JEM 2000 EXII) and a field emission scanning electron microscope (FESEM, JEOL JSM 6700 F, Japan) using exfoliated sections of the printed paper. Fig. 2a and b shows TEM and SEM images, respectively, of the AuNPs on paper at the edges of the pattern. The AuNP density is not very high possibly due to reactant diffusion. However, the SEM from the pattern-edge helps to get a size distribution of the AuNPs. Fig. 2c shows a typical SEM image at pattern-centers which had higher AuNP density and could explain the Raman results. A series of TEM and SEM images were then used to obtain the AuNP size distribution (Fig. 2d) which peaked around 30 nm. The images indicate the formation of AuNPs not only on the surface of the paper but also embedded in it. The UV-VIS spectra (Fig. 2e) (JASCO V-670, JASCO Corp., Japan) show the characteristic surface plasmon band of AuNP at 540 nm (red curve) on the purple region. The small red shift of the absorption band from 520 nm indicates some larger AuNPs or more possibly some agglomeration. This result is consistent with the size distribution observed from the SEM/TEM measurements. In the absence of the AuNPs, on the white portion of the plain paper, there are obviously no absorption bands (black curve, Fig. 2e).

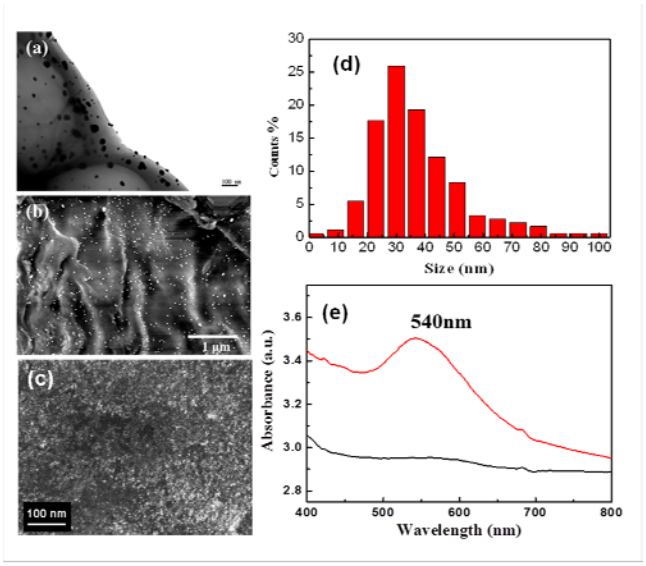

Fig. 2. Typical (a) TEM and (b) SEM images of the AuNPs grown *in situ* on the printed paper at the edge of the pattern. (c) SEM of the AuNPs at the central part of the pattern. (d) Particle size distribution of the AuNPs estimated from the electron microscopy images. (e) UV-VIS spectrum of (top curve, red) the AuNPs printed on paper forming the SERS strips, and (bottom curve, black) the plain paper.

In the current study, the density of the AuNPs are not as high as given by the $d=2r$ condition[40] (Fig. 2a-c), nor is their size as small as 10 nm overall to have the AuNP plasmon absorption peak at 520 nm. Hence there is a scope for further

optimization of the AuNP density. The AuNP size distribution and more importantly its density will depend upon the reactant concentration. Hence there is a need to optimize the SERS strip for sensitivity. The optimization steps, via change of reactant concentrations, are shown in Fig. S2 (ESI†) through which we arrived at a concentration of 2 mM for $HAuCl_4$, and 25 mM for lecithin for the preparation of our SERS strip, as concentration of KI was fixed at 100 mM. The use of a low concentration for $HAuCl_4$ is similar to what is generally used for the preparation of a colloidal solution that looks wine red in colour. Higher concentrations of $HAuCl_4$ would result in larger AuNPs and severe agglomeration (inset c, Fig. S2 (ESI†)). A smaller concentration of lecithin is required for two reasons. First, lecithin solution is sticky and easy to clog the printer head. Heavy deposition of lecithin would invariably result in precipitates on the printed patterns and appear dark after developing (inset c, Fig. S2 (ESI†)). Hence, the dark colour of the patterns, though looks more distinct, are actually inferior to the low contrast pink-purple patterns for SERS functionality.

3 Sensing performance of the SERS strips and its use in food screening

3.1 General calibration of the SERS strip

For a basic understanding of the SERS performance of the strips, 20.0 µL of an aqueous solution of standard molecule Rhodamine 6G (R6G, 99%, Acros, Belgium), at different concentrations, were dispersed on to the SERS strips using a micropipette. The SERS measurements were done using a HR 800 (Jobin Yvon, USA) commercial Raman spectrometer with 632 nm (He–Ne laser, beam diameter ~2µm, 10 mW) excitation. Experimental conditions use a single collection with exposure time between 3-30 s. The RS data of the plain paper (Fig. 3a i), and the AuNP pad on the paper (Fig. 3a ii), is shown in Fig. 3b i and ii, respectively. These two spectra constitute our background signal which is reasonably clean. The fact that the background signal from the paper or the AuNP pads is clean (Fig. 3b i, ii) is extremely useful else it would interfere with the analyte signal.

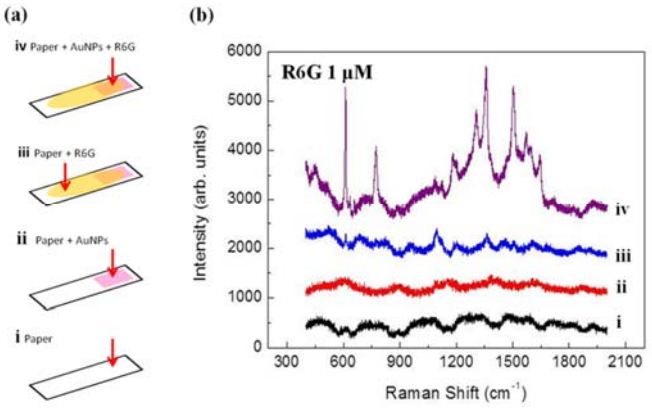

Fig. 3. (a) Schematic illustrations of the SERS experiments performed on the AuNP strips with Rhodamine 6G as the analyte. i) Plain paper; ii) paper with the AuNP pad; R6G dispersed on the strip and measured on the iii) paper, and iv) AuNP pad. b) Corresponding Raman spectra obtained at each stage shown in (a).

The analyte, a solution of 1 µM R6G, is then detected on the strip. The RS and SERS spectrum obtained from the white paper with R6G (Fig. 3a iii), and from the AuNP pads containing R6G (Fig. 3a iv) is shown in curve iii and iv of Fig. 3b, respectively. Curve iii (Fig. 3b) demonstrates weak R6G signals. However, curve iv (Fig. 3b) shows strong fingerprint signals of R6G, at 612, 774, 1363 and 1510 cm^{-1}, due to the presence of AuNPs on the purple pad.

In addition, concentration dependent SERS (on the AuNP paper) and conventional RS (on the plain paper) measurements have been done to check the sensitivity and is presented in Fig. S3 (ESI†)**.** This demonstrates the SERS activity of the strips. The relative standard deviation (*RSD*= standard deviation/ mean) curve, shown at the bottom of each panel in Fig. S3 (ESI†), is used to estimate the reproducibility of the SERS signals and is calculated by a method reported previously.[41] A flat *RSD* would imply the best reproducibility. The *RSD* values for R6G were ~15%, which needs to be improved. This is where the lithographically prepared substrates with precise control of the nanostructure morphology and density are ahead of the SERS strips. But, as mentioned earlier, with maximization of the AuNP density on the paper, this problem can be resolved.

3.2 Performance of the SERS strip in detecting toxic food contaminants

For real use of these SERS strips as a tool for varied molecular detection in drug administration, forensic science, or food-safety protocols, it is imperative to study its sensitivity and reproducibility using relevant molecules and their concentrations. For this purpose our choice was Malachite Green (MG) (Fig. S4 (ESI†)), a common fungicide used in marine animal culture; and Iprodione (Fig. 4**)** a pesticide commonly used in fruits and vegetables, to prevent Botrytis bunch rot, all over the world. Iprodione has low solubility in water, and hence farmers use a modified Iprodione (50%) solution to spray on their crops. Here, we have used this modified real agricultural product (50% Iprodione, Wonderful Agriculture (VN) Co. Ltd., Long An Province, Vietnam) solution for our sensing. A concentration controlled aqueous solution of the real agricultural product was sprayed on the surface of oranges, and thereafter collected by rubbing the SERS strips on the fruit surface. For MG, the solution was drop-coated. The SERS strips were then dried in nitrogen flow. The experimental design includes repeated measurement of different concentrations of these molecules at five different locations on the optimized AuNP pads, and on the plain paper. The repeated measurements would help us obtain the *RSD*.

Fig. 4 & S4 (ESI†) shows the comparison of SERS (panels a- e), measured on the AuNP pads, and the corresponding RS data (panels f- j), measured on plain paper, of real agricultural Iprodione, and MG, respectively, at different concentrations. SERS signals of concentration dependent Iprodione (Fig. 4 a-e**)** and MG (Fig. S4 a-e (ESI†)**)** are measured on the AuNP pads**,** shows increasing intensities with increasing concentration. However, individual SERS intensities are higher than the corresponding RS intensities shown in the adjoining panels (Fig. 4, S4 (ESI†), panels f-j). The diagnostic peak for the agricultural Iprodione is at 998 cm^{-1} (Fig. 4). There is evidence of fluorescence from the analytes, especially at 800 cm^{-1} for Iprodione. These signals had a larger line width and not due to RS. In these cases also, the efficacy of the SERS strip is demonstrated and the analytes could be detected at low concentrations.

Each country has its own rule for the maximum allowed levels of such toxic food additives measured in 'maximum residue levels (MRL)'. The MRL values of MG and Iprodione for the European Union (EU) is 1ppb, and 10 mg/kg, respectively. From the results shown in Fig. 4 & S4 (ESI†), the limit of detection

(LoD) for Iprodione and MG were 10 μM, and 1 nM, respectively, which were below the MRL of the European Union (EU). The LoD was determined experimentally as the concentration at which the analyte signals were detectable with a spectral signal to noise ratio (S/N) equal to or more than 3.0. The data shown in Fig.4e, and Fig S4e, for Iprodione and MG, respectively, are the lowest concentrations measured with S/N ratio >3, and hence the LoD in our case. Although we believe that the AuNP density and the sensitivity of the SERS strips could be further increased, but the current sensitivity levels, of at least the MRL for these molecules, are practically and commercially acceptable.

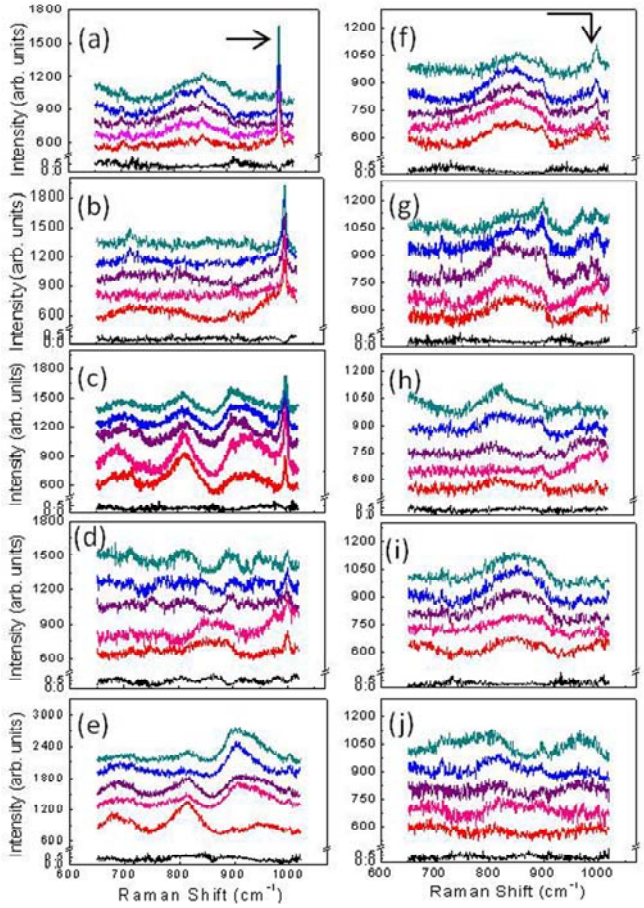

Fig. 4. SERS spectra of real agricultural Iprodione (50%) with different concentrations on the AuNPs: (a) 1 M (b)1x10^{-2} M (c)1x10^{-3} M (d)1x10^{-5} M (e)1x10^{-6} M, collected from 5 randomly selected points on the purple part of the SERS strip (with AuNPs). (f-j) Corresponding Raman scattering (not SERS) spectra of concentration dependent (same as in a-e) Iprodione on the white part of the SERS strips (without AuNPs). The *RSD* (standard deviation/mean) of the 5 spectra are shown at the bottom of each plot in black. The acquisition time for (a-e) is 6 s, whereas for (f-j) is 30 s. The arrows indicate Iprodione peak position.

Fig. 5 shows the variation of the prominent peaks of the analyte molecules (R6G, MG, and Iprodione) as a function of their concentrations when measured on the AuNPs and on plain paper, i.e., for the SERS and RS cases, respectively. To start with, Fig. 5a shows the variation of the 610 cm^{-1} line of R6G as a function of its concentration (Fig. S3 (ESI†)) and fitted with the Langmuir adsorption equation. Fig. 5b and c shows the variation of the 1613 cm^{-1} line of MG, and the 998 cm^{-1} line of Iprodione, respectively, as a function of its concentration. The Langmuir equation relates the coverage or adsorption of the molecules on a solid surface to its concentration, with which the SERS and RS intensities vary, at a fixed temperature. The nice fit to the data indicates good correspondence of the experimental and theoretical predictions of concentration dependent studies. When plotted on a log scale the concentration dependent SERS signals yield a linear variation (Fig. S5a-c (ESI†)). At low analyte concentrations, expressing sub-monolayer adsorption, the signal increases rapidly with increasing concentration (Fig. 5a-c). However, at higher concentrations, reaching a state of monolayer coverage or more, the signal saturates. The slope of the curves (Fig. S5a-c (ESI†)) indicate sensitivity of the SERS measurements. Figure 5 includes the data for both SERS, on the AuNP pads, and corresponding RS studies carried out on the plain paper. The comparison clearly indicates the efficacy of the AuNPs used in the SERS measurements.

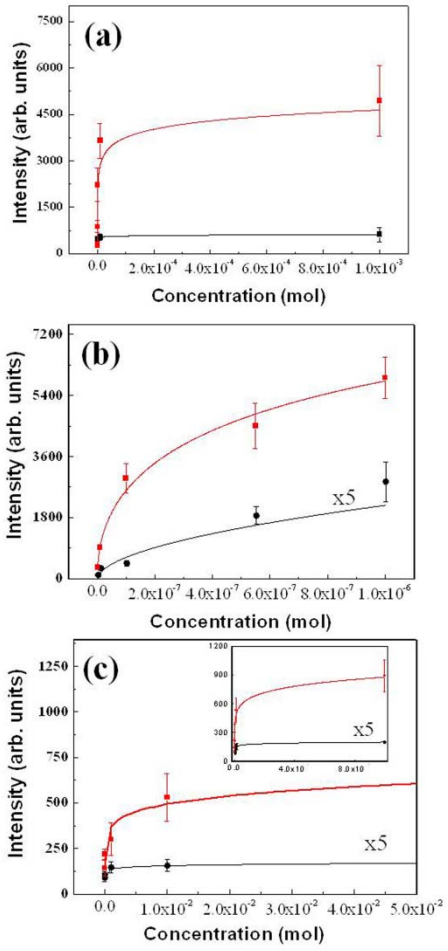

Fig. 5. Variation of the intensity of the signal at (a) 610 cm^{-1} of R6G, (b) 1613 cm^{-1} of Malachite Green, and (c) 998 cm^{-1} of Iprodione, as a function of their respective concentrations plotted in linear scale. Raman (black curve) (measured without AuNPs) and SERS (red curve) (measured with the AuNPs) signals are compared in each plot to show the efficacy of the AuNPs. Inset in (c) shows the same variation over the whole range of concentration studied. The lines joining the data points are a fit according to Langmuir adsorption equation. The error bars indicate standard deviations of five independent measurements.

3.3 SERS mapping

Lastly, SERS mapping was done to demonstrate molecular imaging on the strips. All the above molecules used for detection could be used for the purpose, however, here we chose two kinds

of fluorescent dyes, frequently used in cell staining, i) Fluorescein, and ii) Nile Red. This is to demonstrate the versatility of the AuNP strip against a strong fluorescence that normally suppresses the Raman signals. 100 μM solutions of these dyes were dispersed on plain paper (as control) and the AuNP pads. RS was performed to select specific features to scan for. An area of 10 μm x 10 μm was scanned for each sample to map the intensity of the specific Raman features from the chosen dyes, under same experimental conditions. The sample stage had a X-Y resolution of ~0.7 μm.

The results of the Raman mapping of fluorescein (~1540 cm^{-1} band) on plain paper (Fig. 6a) and the AuNP pads (Fig. 6b) are presented. A similar data for Nile Red can be found in Fig. S6 (ESI†). As expected, the AuNP pads show remarkably enhanced and distinct molecular imaging, compared to the plain paper, at the given concentration of the dye dispersion which is assumed identical on the two surfaces. The pixel intensity (Fig. 6) is a function of the number of dye molecules as well as the AuNP aided enhancement at that location. The SERS strips, along with its potential to be used as a molecular mapping surface, add strength to the emerging field of paper based devices for biological assays.[36,42,43]

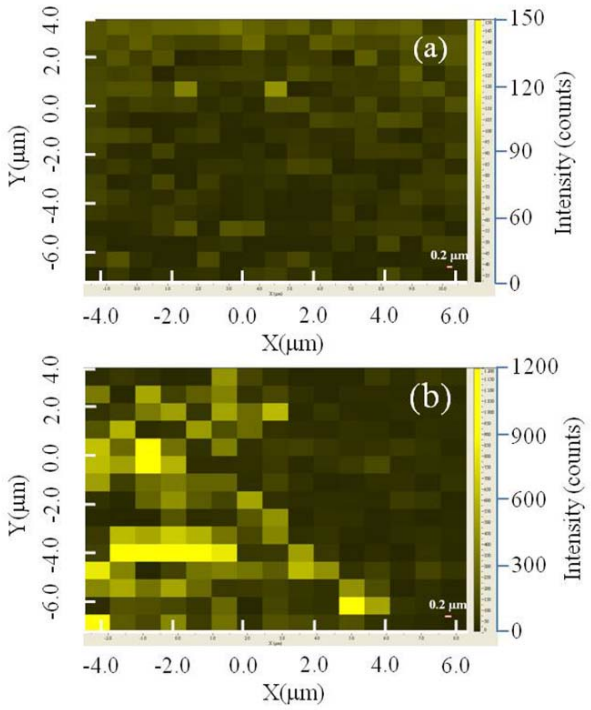

Fig. 6. SERS mapping for molecular imaging of Fluorescein, 100 μM, on (a) plain paper, and (b) AuNP pad.

4 Conclusions

In summary, we have demonstrated the facile fabrication and use of a flexible SERS strip for possible on-site toxicity screening of food and drinks. The SERS strip is made on plain printing paper by ink-jet printing. A combination of lecithin and potassium iodide is used to reduce chloroauric acid at room temperature. The gold NPs are formed *in-situ* on the printed patterns. The SERS strips demonstrate reasonably high sensitivity for the detection of common Raman active molecules, as Rhodamine 6G, and toxic materials in food, such as Malachite Green, and Iprodione. The method is scalable with potential for use in other kind of printing materials. The flexible paper substrate is free of background Raman signals or fluorescence, and, we believe, its porous nature helps in holding the toxic analytes when rubbed on the surface of fruits/vegetables, not readily possible for rigid substrates, for subsequent detection via SERS.

Acknowledgment

The authors would like to acknowledge financial support from National Science Council, Grant Nos. (NSC-101-2112-M-010-003-MY3, and 101-2120-M-001-010), and Aim of Top University plan of MoE, Taiwan.

Notes and references

[*a] *Institute of Biophotonics, National Yang Ming University, 155, Sec-2, Li-Nong Street, Taipei-112, Taiwan. Tel: +886 2 28267909; Fax: +886 2 2823 5460. E-mail: sur@ym.edu.tw;*

[b] *Biophotonics and Molecular Imaging Research Center, National Yang Ming University, Taipei-112, Taiwan.*

† Electronic Supplementary Information (ESI) available: [Fabrication and optimization procedures of the SERS strips; SERS and conventional Raman scattering data for Malachite Green, and Rhodamine 6G on the SERS strip and paper; SERS mapping of Nile Red on the SERS strip].

1 R.Aroca, Surface Enhanced Vibrational Spectroscopy, *John-Wiley & Sons, Toronto*, 2006.
2 S. Nie and S. R. Emory, Probing Single Molecules and Single Nanoparticles by Surface-Enhanced Raman Scattering, *Science*, 1997, **275**, 1102.
3 E. Katz and I. Willner, Integrated Nanoparticle–Biomolecule Hybrid Systems: Synthesis, Properties, and Applications, *Angewandte Chemie International Edition*, 2004, **43**, 6042.
4 M. Moskovits, Surface-Enhanced Spectroscopy, *Reviews of Modern Physics*, 1985, **57**, 783.
5 T. Vo-Dinh, H.-N. Wang and J. Scaffidi, Plasmonic Nanoprobes for SERS Biosensing and Bioimaging, *Journal of Biophotonics*, 2010, **3**, 89.
6 A. G. Brolo, E. Arctander, R. Gordon, B. Leathem and K. L. Kavanagh, Nanohole-Enhanced Raman Scattering, *Nano Letters*, 2004, **4**, 2015.
7 B. Liu, M. Lin and H. Li, Potential of SERS for Rapid Detection of Melamine and Cyanuric Acid Extracted from Milk, *Sens. & Instrumen. Food Qual.*, 2010, **4**, 13.
8 J. F. Li, Y. F. Huang, Yong Ding, Zhi Lin Yang, Song Bo Li, Xiao Shun Zhou, Feng Ru Fan, Wei Zhang, Zhi You Zhou, De Yin Wu, Bin Ren, Zhong Lin Wang & Zhong Qun Tian, Shell-Isolated Nanoparticle-Enhanced Raman Spectroscopy, *Nature* , 2010, **464**, 392.
9 D. A. Handley, Methods for Synthesis of Colloidal Gold. In Gold:Principles, Materials and Applications, *Hayat, M., A., Ed; Academic Press, Inc.: New York 1*, 1989, 13.
10 S. Panigrahi, S. Kundu, S. Ghosh, S. Nath and T. Pal, General Method of Synthesis for Metal Nanoparticles, *Journal of Nanoparticle Research*, 2004, **6**, 411.
11 J. Wagner, T.Tshikhudo, J.Koehler, Microfluidic Generation of Metal Nanoparticles by Borohydride Reduction, *Chemical Engineering Journal,* 2008, **135**, S104-S109.
12 I. Hussain, S. Z. Hussain, R. Habib ur, A. Ihsan, A. Rehman, Z. M. Khalid, M. Brust and A. I. Cooper, In Situ Growth of Gold Nanoparticles on Latent Fingerprints-from Forensic Applications to Inkjet Printed Nanoparticle Patterns, *Nanoscale*, 2010, **2**, 2575.
13 S. Chattopadhyay, H.-C. Lo, C.-H. Hsu, L.-C. Chen and K.-H. Chen, Surface-Enhanced Raman Spectroscopy Using Self-Assembled Silver Nanoparticles on Silicon Nanotips, *Chemistry of Materials*, 2005, **17**, 553.
14 S. Chattopadhyay, S. C. Shi, Z. H. Lan, C. F. Chen, K.-H. Chen and L.-C. Chen, Molecular Sensing with Ultrafine Silver Crystals on Hexagonal Aluminum Nitride Nanorod Templates, *Journal of the American Chemical Society*, 2005, **127**, 2820.

15 L. Qin, S. Zou, C. Xue, A. Atkinson, G. C. Schatz and C. A. Mirkin, Designing, Fabricating, and Imaging Raman Hot Spots, *Proceedings of the National Academy of Sciences*, 2006, **103**, 13300.
16 C. L. Haynes and R. P. Van Duyne, A Versatile Nanofabrication Tool for Studies of Size-Dependent Nanoparticle Optics, *The Journal of Physical Chemistry B*, 2001, **105**, 5599.
17 M.E. Hankus, D. N.Stratis-Cullum, P. M. Pellegrino, Surface Enhanced Raman Scattering (SERS)-Based Next Generation Commercially Available Substrate: Physical Characterization and Biological Application, *SPIE-Optics and Photonics West-Biosensing and Nanomedicine IV,* 2011, **8099**, paper 8099-8097.
18 M. Fan, G. F. S. Andrade and A. G. Brolo, A Review on The Fabrication of Substrates for Surface Enhanced Raman Spectroscopy and Their Applications in Analytical Chemistry, *Analytica Chimica Acta*, 2011, 693, 7.
19 X. Zhang, C. R. Yonzon, M. A. Young, D. A. Stuart and R. P. V. Duyne, Surface-Enhanced Raman Spectroscopy Biosensors: Excitation Spectroscopy for Optimisation of Substrates Fabricated by Nanosphere Lithography, In *IEE Proceedings - Nanobiotechnology*, 2005, 195.
20 A. J. Baca, T. T. Truong, L. R. Cambrea, J. M. Montgomery, S. K. Gray, D. Abdula, T. R. Banks, J. Yao, R. G. Nuzzo and J. A. Rogers, Molded Plasmonic Crystals for Detecting and Spatially Imaging Surface Bound Species by Surface-Enhanced Raman Scattering, *Applied Physics Letters*, 2009, **94**, 243109.
21 H.-H. Cheng, S.-W. Chen, Y.-Y. Chang, J.-Y. Chu, D.-Z. Lin, Y.-P. Chen and J.-H. Li, Effects of the Tip Shape on The Localized Field Enhancement and Far Field Radiation Pattern of the Plasmonic Inverted Pyramidal Nanostructures with the Tips for Surface-Enhanced Raman Scattering, *Opt. Express*, 2011, **19**, 22125.
22 G. L. Liu and L. P. Lee, Nanowell Surface-Enhanced Raman Scattering Arrays Fabricated by Soft-Lithography for Label-free Biomolecular Detections in Integrated Microfluidics, *Applied Physics Letters* , 2005, **87**, 074101.
23 K. Nakamoto, R.Kurita, , O.Niwa, 2011, 15th International Conference on Miniaturized Systems for Chemistry and Life Sciences *Seattle, Washington, USA, 1786.*
24 M. C. Netti, M. E. Zoorob, M. D. Charlton, P. Ayliffe, S.Mahnkopf, P. Stopford, K. Todd, J. R. Lincoln, N. M. B. Perney, J. J. Baumberg, 2006, Biomedical Vibrational Spectroscopy III: Advances in Research and Industry, *6093*.
25 F. P. Zamborini, M. C. Leopold, J. F. Hicks, P. J. Kulesza, M. A. Malik and R. W. Murray, Electron Hopping Conductivity and Vapor Sensing Properties of Flexible Network Polymer Films of Metal Nanoparticles, *Journal of the American Chemical Society*, 2002, **124**, 8958.
26 S. H. Ko, H. Pan, C. P. Grigoropoulos, C. K. Luscombe, J. M. J. Fréchet and D. Poulikakos, All-Inkjet-Printed Flexible Electronics Fabrication on a Polymer Substrate by Low-Temperature High-Resolution Selective Laser Sintering of Metal Nanoparticles, *Nanotechnology*, 2007, **18**, 345202.
27 N. D. Luong, J. Oh, Y. Lee, J. H. Yeon, J. Hur, J. J. Park, J. M. Kim and J.-D. Nam, Immobilization of Gold Nanoparticles on Poly, Methyl Methacrylate, Electrospun Fibers Exhibiting Solid-state Surface Plasmon Effect, *Surface and Interface Analysis*, 2012, **44**, 318.
28 K. Jiang, A. Eitan, L. S. Schadler, P. M. Ajayan, R. W. Siegel, N. Grobert, M. Mayne, M. Reyes-Reyes, H. Terrones and M. Terrones, Selective Attachment of Gold Nanoparticles to Nitrogen-Doped Carbon Nanotubes, *Nano Letters*, 2003, **3**, 275.
29 A. Määttänen, P. Ihalainen, P. Pulkkinen, S. Wang, H. Tenhu and J. Peltonen, Inkjet-Printed Gold Electrodes on Paper: Characterization and Functionalization, *ACS Applied Materials & Interfaces*, 2012, **4**, 955.
30 I. Park, S. H. Ko, H. Pan, C. P. Grigoropoulos, A. P. Pisano, J. M. J. Fréchet, E. S. Lee and J. H. Jeong, Nanoscale Patterning and Electronics on Flexible Substrate by Direct Nanoimprinting of Metallic Nanoparticles, *Advanced Materials*, 2008, **20**, 489.
31 C.-L. Zhang, K.-P. Lv, H.-P. Cong and S.-H. Yu, Controlled Assemblies of Gold Nanorods in PVA Nanofiber Matrix as Flexible Free-Standing SERS Substrates by Electrospinning, *Small*, 2012, **8**, 648.
32 D. He, B. Hu, Q.-F. Yao, K. Wang and S.-H. Yu, Large-Scale Synthesis of Flexible Free-Standing SERS Substrates with High Sensitivity: Electrospun PVA Nanofibers Embedded with Controlled Alignment of Silver Nanoparticles, *ACS Nano*, 2009, **3**, 3993.
33 P.M.Fierro-Mercado, S.P.Hernández-Rivera, Highly Sensitive Filter Paper Substrate for SERS Trace Explosives Detection, *International Journal of Spectroscopy*, 2012, **2012**, 7.
34 A. J. Chung, Y. S. Huh and D. Erickson, Large Area Flexible SERS Active Substrates Using Engineered Nanostructures, *Nanoscale*, 2011, **3**, 2903.
35 Y. Zhao, Toward practical SERS sensing, 2012, *Proc. of SPIE 8401*. Independent Component Analyses, Compressive Sampling, Wavelets, Neural Net, Biosystems, and Nanoengineering X, 84010O (May 1, 2012); doi:10.1117/12.918761.
36. M. Li, J. Tian, M. Al-Tamimi, W. Shen, Paper Based Blood Typing Device that Reports Patient's Blood Type 'In Writing', *Angew. Chem. Intl. Ed*., 2012, **51**, 5497.
37 J. J. Laserna, A. D. Campiglia, J. D. Winefordner, Mixture Analysis and Quantitative Determination of Nitrogen-Containing Organic Molecules by Surface-Enhanced Raman Spectrometry, *Analytical Chemistry,* 1989, **61**, 1697.
38 W. W. Yu, I. M. White, Inkjet Printed Surface Enhanced Raman Spectroscopy Array on Cellulose Paper, *Analytical Chemistry,* 2010, **82,** 9626.
39 L. L. Qu, D. W. Li, J. Q. Xue, W. L. Zhai, J. S. Fossey, and Y. T. Long, Batch fabrication of disposable screen printed SERS assays, *Lab on a Chip*, 2012, **12**, 876.
40 F. J. García-Vidal and J. B. Pendry Collective Theory for Surface Enhanced Raman Scattering, *Physical Review Letters*, 1996, **77**, 1163.
41 P. K. Roy, Y.-F. Huang and S. Chattopadhyay, Detection of Melamine on Fractals of Unmodified Gold Nanoparticles by Surface-Enhanced Raman Scattering, *Journal of Biomedical Optics*, 2013, **19**, 011002.
42. X. Mu, L. Zhang, S. Chang, W. Cui, Z. Zheng, Multiplex Microfluidic Paper-based Immunoassay for the Diagnosis of Hepatitis C Virus Infection, Analytical Chemistry, 2014, **86**, 5338.
43. A. Apilux, Y. Ukita, M. Chikae, O. Chailapakul, Y. Takamura, Development of Automated Paper-Based Devices for Sequential Multistep Sandwich Enzyme-Linked Immunosorbent Assays Using Inkjet Printing, *Lab. Chip*., 2013, **13**, 126.

An ink-jet printed surface enhanced Raman scattering paper for food screening.†

W. J. Liao,[a] Pradip K. Roy, S. Chattopadhyay [a,b*],

Graphical Abstract:

A surface enhanced Raman spectroscopy active strip, with gold nanoparticles, is developed on paper by ink-jet printing for toxic screening.